L0MDT Progress Report

Riley Gleason (University of California, Irvine)

March 31, 2024

1) Introduction

The Large Hadron Collider (LHC) has deepened our understanding of particle physics and aims to further this by increasing its instantaneous luminosity to provide a substantial dataset (3000 fb^{-1}). Consequently, detectors like ATLAS will have to manage increased occupancy due to the increased pileup and must be enhanced to maintain the physics goals. The first level trigger system must also be improved to handle the increased rate, while maintaining excellent efficiency and large background rejection.

To address this, a major overhaul of the ATLAS detector and trigger system, focusing on upgrading the trigger system with advanced algorithms for particle identification, and event reconstruction, must be made to ensure detector performance. The UCI group is spearheading the development of the Level-0 Monitored Drift Tubes (L0MDT) trigger and readout system. This project aims to utilize the Monitored Drift Tubes (MDT) data in the muon trigger decision, to identify and select potential muon track candidates based on simplified information from the muon chambers. This only became feasible due to the increased latency for the Level-0 trigger decision in the High-Luminosity LHC era. MDTs offer improved accuracy in muon track determination compared to other muon trigger detectors. Consequently, they can enhance muon trigger selection capabilities by decreasing the occurrence of false muon triggers, effectively managing the muon trigger rate.

The L0MDT system consists of 64 Advanced Telecom Computing Architectures (ATCA) blades, each dedicated to a sector, featuring large Field-Programmable Gate Arrays (FPGAs) and high-speed optical links. These blades manage configuration, control, and monitoring of MDT front-end electronics, and perform trigger functionalities [1]. The focus in the coming years will be on validating hardware and firmware, integrating L0MDT with MDT front-end electronics and ATLAS DAQ, enhancing the muon trigger system, and developing monitoring capabilities.

One of my initial project goals was to take ownership of the algorithm responsible for linking muon segments to measure muon p_T, aiming to improve the resolution. The transverse momentum resolution is defined as

$$\sigma = \frac{p_T^{On} - p_T^{Off}}{p_T^{Off}} \tag{1}$$

p_T^{Off} represents offline transverse momentum, while p_T^{On} refers to the online counterpart. Online reconstruction takes place in real-time, while offline reconstruction involves processing stored data to ensure high accuracy. This improvement was accomplished by adjusting both the code and the fit procedure to extract p_T^{On}.

The next step was to propagate the updates made in the L0MDTTrigger into L0MDT firmware and validate them. New Look-Up Tables (LUTs) were created, and I am now in the process of running those through High-Level Synthesis (HLS) for use in FPGAs. Additionally, I developed an option which allows for a significant decrease in the number of parameters the LUTs hold.

Finally, I am in the process of creating a web-based graphical interface to streamline interaction with L0MDT while validating the functionalities and performance of the firmware. It will support

physicists and engineers during testing and validation by functioning as an easy-to-use debugging tool for the L0MDT system within the ATLAS experiment throughout production, installation, commissioning, and final operation.

2) Implementation of p_T Calculation in L0MDT

The precise determination of particle properties at the trigger level is important for our objective of gathering accurate data and controlling the trigger to be within the available data bandwidth. Utilizing precise position measurements within the bending plane of the MDT chambers in the ATLAS detector, the MDT trigger algorithm reconstructs the trajectory of muons as they pass through these chambers.

Following these position measurements, the algorithm initiates the reconstruction of a segment within each chamber, representing straight tracks. By analyzing variance in position and angle at Inner (I), Middle (M), and Outer (O) stations, we map the curvature of the muon influenced by magnetic fields, providing the path and groundwork for precise determination of transverse momentum (p_T). Then, based on this measurement, the decision whether to accept or reject this muon candidate for a given p_T trigger threshold is made.

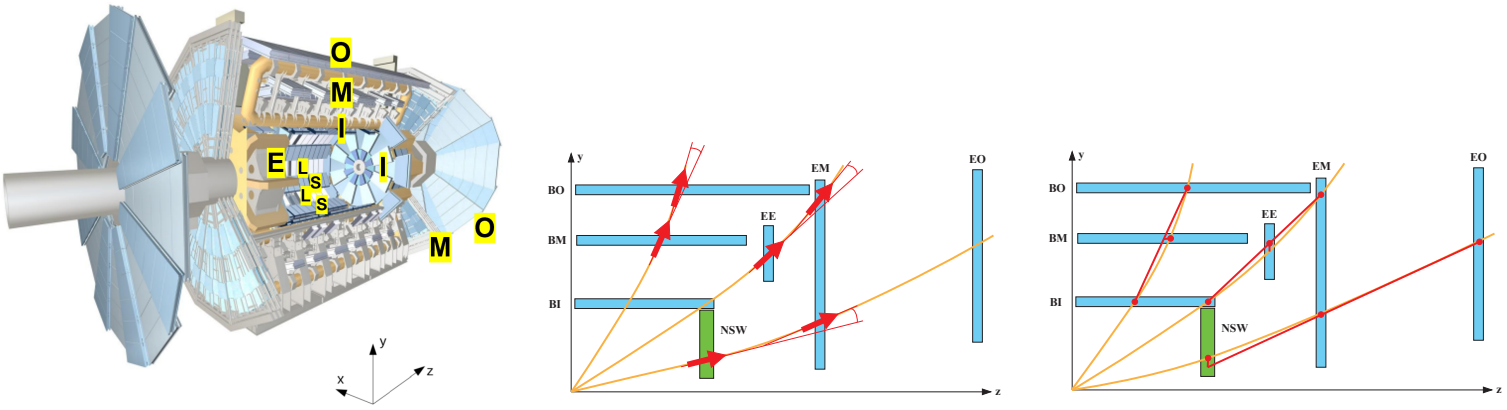

Fig 1: The left is the ATLAS Muon Spectrometer, containing 16 sectors in ϕ. L indicates Large sectors; S is Small sectors. Inner (I), Middle (M), Outer (O), and Extra (E) stations are indicated. The middle depicts the 2 segments, deflection angle method, while the right shows the 3 segments, sagitta. [2].

A major goal was the improvement of the resolution as a function of the absolute value of the pseudorapidity (η). This was achieved by refining the fit procedures that are used to calculate the muon's p_T^{On}. There are two ways for the p_T^{On} to be calculated. If 2 segments are reconstructed, then the method that is used is called the deflection angle, as it depends on the difference in polar angle between the track segments enables the calculation of p_T^{On}. By assuming the deflection angle is small, knowing the field strength, and the distance between segments you arrive at the equation below.

$$p_T = \frac{eBL}{\beta} \tag{2}$$

If 3 segments are reconstructed, then the sagitta method would be used.

$$p_T = \frac{0.3L^2B}{8S} \tag{3}$$

By comparing equations (2) to (3) you can see that the deflection angle is dependent on the accuracy of the angle of the reconstructing segments, while the sagitta is dependent on the position reconstruction. Both quantities, deflection angle and sagitta, are inversely proportional to p_T. However, to account for the complex variation of the magnetic field through the detector, the fitting procedure to extract the relationship between the sagitta/deflection angle and p_T needs to be segmented regionally. In addition, an iterative fitting procedure needs to be used to correct for the variation in the magnetic field along ϕ and η. The final parametrization, adjusted for magnetic field variation, is below.

$$p_T \approx \frac{\left(\frac{1}{s} - a_0\right)}{a_1} + \sum_{i=0}^{2} p_i \phi_{mod}^{i} + \sum_{i=0}^{1} e_i |\eta^i| \tag{4}$$

After iterative fitting, you obtain a_0 and a_1 from the linear fit $y = mx + b$ of $\frac{1}{|S|}$ vs. p_T^{Off}. For p_i, use a quadratic fit broken into 3 linear fits, and for e_i, use a quadratic fit broken into only 2 linear fits due to the absolute value.

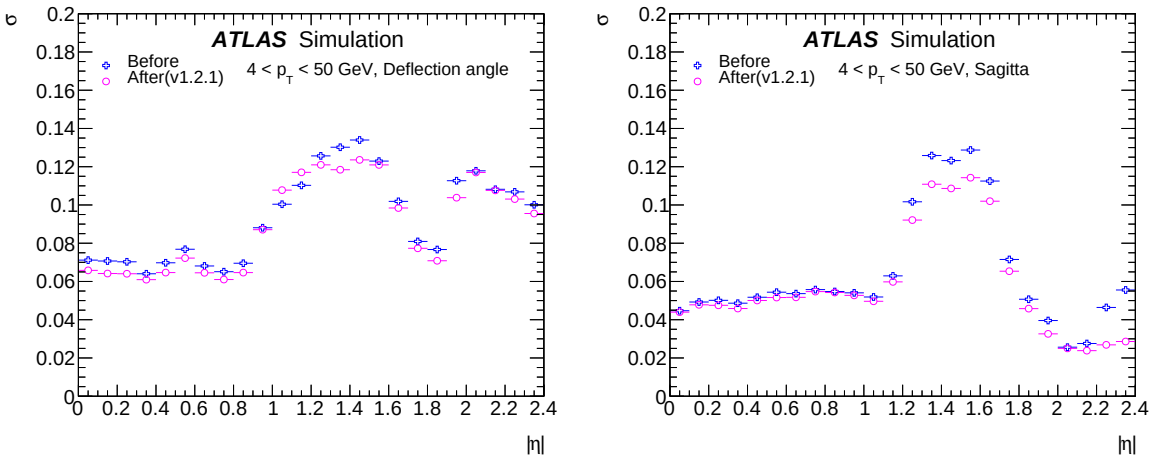

Fig 2: These show the resolution vs $|\eta|$. Where blue was the initial result and pink contains my updates. The left is 2 segments (Deflection angle), and the right is 3 segments (Sagitta). On the x-axis, Barrel region spans from 0 to 1.05, Transition from 1.05 to 1.3, and Endcap from 1.05 to 2.4.

Furthermore, I have incorporated a function into the algorithm, for measuring muon p_T, to reduce the regional segmentation of the fit procedure, effectively decreasing it by a factor of 6. However, this modification introduces challenges because splitting the regions effectively divides the data into areas with potentially different behaviors which can help identify local structures or patterns that may not be apparent when examining at the entire range. Nevertheless, this still offers advantages, such as more statistical data for fitting within each region. Every region undergoes a parameterization process, requiring the precise determination of up to 7 parameters (equation 4) to accurately calculate p_T^{On}. Consequently, a greater number of regions would result in more data that must be stored in LUTs, which are memory units storing pre-computed output values for every possible combination of input values. As FPGAs have finite resources, making efficient use of these resources allows for more functionality to be packed into a single device. This function decreases the total number of parameters from 1948 to 327. This significant reduction in parameters decreases the footprint in an FPGA.

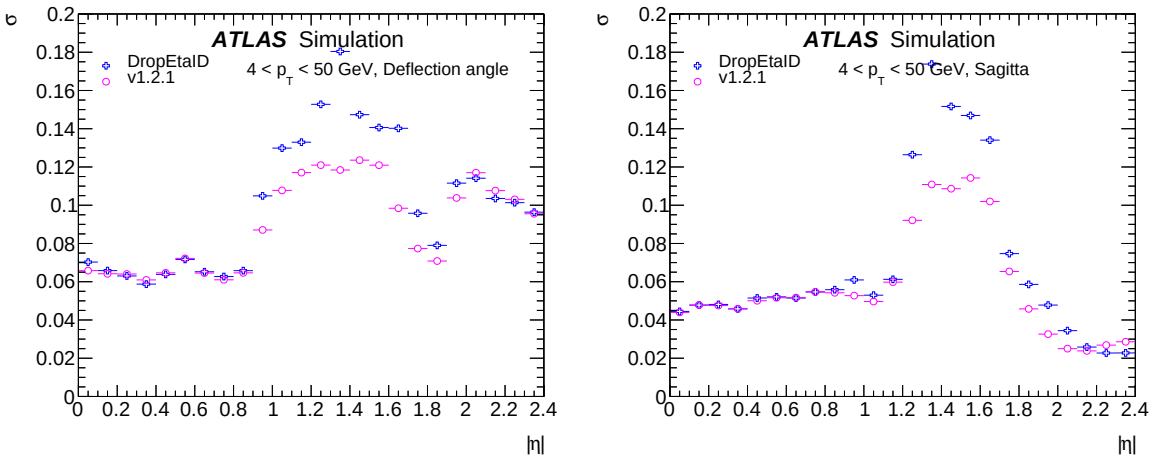

Fig 3: All depict the resolution vs $|\eta|$. Here, blue represents the parameterization with fewer regions, while pink, identical with Figure 2 (v1.2.1), includes it.

The figures above reveal that, apart from the increase in resolution at the Transition and early Endcap regions, the blue points, with fewer regions, now closely matches the pink. This represents a significant improvement compared to when I initially implemented and executed this function, where the highest point for the resolution was 0.27. The issue arises because in the transition region, the magnetic field weakens and becomes less uniform due to the transition from the Barrel toroid to the Endcap toroid, compromising the accuracy of p_T measurement. The next steps for this project will involve improving the resolution further in the transition region and generating LUTs, followed by putting it through High-Level Synthesis (HLS).

3) HLS-p_T

The next step involves propagating the updates made to algorithm to the L0MDT firmware and validating them. Currently, I am in the process of taking the newly derived LUTs and running them through HLS.

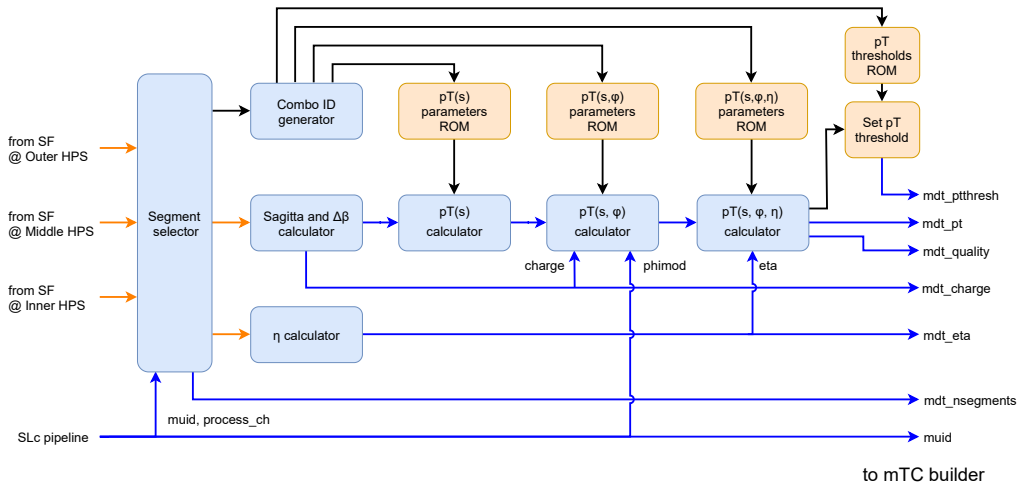

Fig 4: The p_T calculation block in HLS firmware

To clarify, HLS translates high-level functional descriptions, such as C++, into detailed Register Transfer Level (RTL) micro-architectures, like Verilog. These RTL outputs are synthesizable into FPGA bitstreams, enabling on-board execution. Comparing the HLS code output with the offline-generated Test-Vectors (TV) allows us to validate the Firmware (FW) implementation. The result will be updated firmware for the L0MDT boards, aiding in track candidate confirmations [3]. These are the improvements I will be making to the p_T calculation block in HLS firmware.

4) Monitoring

I am developing a web-based graphic interface which will be a user-friendly front-end application to simplify interaction with L0MDT hardware. The goal is to make this tool available to physicists and engineers that will be performing the testing and validation of the L0MDT hardware across various test benches. This tool will also function as a low-level tool for experts to debug issues during the long-term operation of the L0MDT system in the ATLAS experiment. It will offer comprehensive control over board status, encompassing tasks such as programming the FPGA, configuring L0MDT firmware and MDT front-end electronics, validating optical links to neighboring systems, testing and debugging firmware execution, and monitoring firmware to report errors. Finally, the WebGUI will serve as a testing interface for all firmware components of the board. Currently, it enables programming the FPGA, conducting read/write operations on registers, and analyzing data between blocks using SpyBuffer functions. SpyBuffers provide access to signals within the FPGA without affecting the circuit's functionality, allowing users to capture signals at specific points in the design for external analysis. Over the next few months, I aim to significantly enhance both its capabilities and functionalities.

References

1. ATLAS Collaboration. *Technical Design Report for the Phase-II Upgrade of the ATLAS TDAQ System*. Tech. rep. CERN-LHCC-2017-020. ATLAS-TDR-029. Geneva: CERN, Sept. 2017. URL: `https://cds.cern.ch/record/2285584`.

2. ATLAS L0MDTTP Collaboration. ATLAS TDAQ Phase-II Upgrade: Level 0 Muon MDT Trigger Processor Firmware Specification and Design. Tech. rep. Geneva: CERN, 2023. URL: `https://cds.cern.ch/record/2800555`

3. P. Sundararajan, A. Taffard, J. Wollrath, K. Ntekas, J. Olsson. *L0MDT Firmware Test Infrastructure Using CocoTB*. URL: `https://indico.cern.ch/event/1087320/contributions/4570916/attachments/2328305/3966812/L0MDT_firmware_test_framework.pdf`.